Structural and Optical Properties of Silver-Doped Zirconia and Mixed Zirconia−Silica Matrices Obtained by Sol−Gel Processing

F. Gonella, G. Mattei,* and P. Mazzoldi

INFM, Dipartimento di Fisica, Università di Padova, via Marzolo 8, I-35131 Padova, Italy

G. Battaglin

INFM, Dipartimento di Chimica Fisica, Univerità di Venezia, Calle Larga S. Marta 2137, I-30123 Venezia, Italy

A. Quaranta

INFM-Padova, Dipartimento di Ingegneria dei Materiali, Università di Trento, via Mesiano 77, I-38050 Trento, Italy

G. De

Sol-Gel Division, Central Glass and Ceramic Research Institute, 196, Raja S.C. Mullick Road, Calcutta 700032, India

M. Montecchi

ENEA-Casaccia, via Anguillarese, Roma, Italy

Received September 25, 1998. Revised Manuscript Received December 29, 1998

The annealing behavior of zirconia and mixed zirconia−silica matrices (with different ZrO_2/SiO_2 molar ratios) containing silver nanoclusters, synthesized by the sol−gel technique has been investigated. The film samples of the general formula $(SiO_2)_x(ZrO_2)_{(0.9-x)}Ag_{0.1}$ ($x = 0$, 0.225, 0.45, 0.675, and 0.9) were treated in different atmospheres (air, N_2, and $5\%H_2-95\%N_2$) at temperatures ranging from 200 to 900 °C. The ZrO_2 matrix undergoes a structural phase transition from amorphous to cubic-tetragonal polycrystalline between 400 and 500 °C and on further raising the temperature near 600−700 °C the monoclinic phase also develops. On the contrary, the ZrO_2:SiO_2 system remains amorphous up to ∼700 °C. Ag nanoclusters are formed in all the systems. It has been observed that the change in the ZrO_2/SiO_2 molar ratio is an effective way to control not only the overall refractive index of the matrix but also the Ag cluster size. The shifting of the surface plasma resonance position of Ag nanoclusters is observed as a function of the refractive indices of the matrix following the Mie theory. Samples where characterized by transmission electron microscopy, Rutherford backscattering spectrometry, and optical spectrometry to correlate the cluster structure to their optical properties.

1. Introduction

The increasing interest in the fabrication of glass-based composite materials for optical applications has conveyed a great deal of work, aimed from the technological point of view to develop nonlinear optical systems (to be used for instance as all-optical switching devices[1]) and from the theoretical side to the comprehension of the fundamental properties of strongly confined electronic systems, like semiconductor or metallic nanometric-sized quantum dots embedded in dielectric matrices. It is well-known indeed that the presence of nanoclusters inside the matrix enhances the third-order electronic susceptibility $\chi^{(3)}$ of the host by several orders of magnitude (the second-order one being zero for the centrosymmetric nature of the resulting composite). This reflects from a phenomenological point of view in the development of a refractive index n which depends on the intensity I of the laser field used to excite the system as $n = n_0 + n_2 I$, where n_0 is the linear contribution and n_2 is related to the real part of $\chi^{(3)}$.[2,3] Such

* Corresponding author. Fax: +39-049-8277003. E-mail: mattei@padova.infm.it.

(1) Vogel, E. M. *J. Am. Ceram. Soc.* **1989**, *72*, 719.

(2) Mazzoldi, P.; Arnold, G. W.; Battaglin, G.; Gonella, F.; Haglund, R. F., Jr. *J. Nonlin. Opt. Phys. Mat.* **1996**, *5*, 285.

(3) Butcher, P. N.; Cotter, D. *The Elements of Nonlinear Optics*; Cambridge University Press: Cambridge, U.K., 1990.

10.1021/cm980749x CCC: $18.00
Published on Web 02/25/1999

properties are very sensitive to the cluster size and dispersion and they can be ascribed to the interplay between an *intrinsic* cluster feature which is the quantum confinement of the delocalized electrons and an *extrinsic* one which is due to the interaction with the matrix. It is well-known that the dipolar optical absorption of a spherical cluster of volume $V_0 = (4\pi/3)R^3$ and size-dependent dielectric function $\epsilon(\omega;R) = \epsilon_1(\omega;R) + i\epsilon_2(\omega;R)$ embedded in a nonabsorbing medium of dielectric constant ϵ_m can be described by the Mie cross-section $\sigma(\omega;R)$ as follows:[4]

$$\sigma(\omega;R) = 9\frac{\omega}{c}\epsilon_m^{3/2}V_0\frac{\epsilon_2(\omega;R)}{[\epsilon_1(\omega;R) + 2\epsilon_m]^2 + \epsilon_2(\omega;R)^2} \quad (1)$$

Looking at the denominator of eq 1 it is obvious that variations in either $\epsilon(\omega;R)$ or ϵ_m may be used to induce a shift in the surface plasma resonance (SPR) of the system. Therefore, in order to exploit linear as well nonlinear optical properties of these composites, one can follow two main approaches which emphasize these two routes in turn: the first one consists in varying, for a given matrix composition (silica, for instance), either the cluster composition or size in order to modify $\epsilon(\omega;R)$. The second approach relies on changing the matrix composition and therefore its dielectric function ϵ_m.

Following the latter approach, in this work we have studied the effect of the matrix composition as a function of the annealing temperature on the structural and optical properties of silver-doped zirconia and mixed zirconia−silica matrices obtained by the sol−gel technique. The interest in zirconia-based systems stems besides from their chemical and mechanical stability[5,6] and also from their high refractive indices, which make them very attractive from an optical point of view, for instance, for active waveguides fabrication.[7] With respect to other widely employed techniques to obtain composite glasses like ion implantation or ion exchange, one of the main advantages of sol−gel processing is that cluster-doped glasses are synthesized in a single technological process: from the point of view of zirconia-mixed oxides, ZrO_2-SiO_2, $ZrO_2-Al_2O_3$, or ZrO_2-TiO_2 systems have been obtained with a high degree of homogeneity.[5,8] In a previous work[9] we reported on the annealing behavior of silver and copper nanoclusters embedded in a sol−gel synthesized SiO_2 matrix. In this paper, we extend the analysis, focusing our attention on the ZrO_2-SiO_2 system to investigate the structural and optical properties of Ag clusters embedded in dielectric matrices whose composition ranges from SiO_2 to ZrO_2 through different ZrO_2/SiO_2 molar ratios so as to obtain different dielectric properties (and therefore refractive indices) for the resulting host.

2. Experimental Section

A partially hydrolyzed silica sol (25 equiv wt % SiO_2) was first prepared in the following way: TEOS (>98%, Fluka) was dissolved in *n*-propanol (50% of the total amount) and to this a solution containing water, nitric acid, and *n*-propanol (remaining 50%) was added with stirring at room temperature (25 °C). The stirring was continued for 6 h. The molar ratio of TEOS:$C_3^nH_7OH$:H_2O:HNO_3 was 1:3.5:1:0.01. Similarly a partially acetylacetonato complexed Zr−*n*-propoxide solution (20 equiv wt % ZrO_2) was prepared in the following way: a propanolic solution of acetylacetone (acac) was added to zirconium−*n*-propoxide (70% solution in *n*-propanol, Fluka) with stirring at room temperature. The molar ratio of Zr-(O^nPr)$_4$:$C_3^nH_7OH$:acac was 1:3.5:0.6. The partially hydrolyzed silica sol and the partially acetylacetonato complexed Zr−*n*-propoxide solution were mixed under stirring to prepare a mixed SiO_2-ZrO_2 sol. To this mixed sol, the desired amount of $AgNO_3$ dissolved in a water−nitric acid−*i*-propanol mixture was added with stirring in the absence of light. The sol was then diluted with the required amount of *n*-propanol to make the total oxide ($SiO_2 + ZrO_2$) content of 5 equiv wt %. Five sets of silver-doped mixed SiO_2-ZrO_2 sols corresponding to the molar ratio of SiO_2:ZrO_2:Ag = x:(0.9−x):0.1 (where x was fixed at the values of 0, 0.225, 0.45, 0.675, and 0.9) were prepared. The concentration of silver and total $SiO_2 + ZrO_2$ (10 mol % Ag/90% ($SiO_2 + ZrO_2$)) was fixed in all the sols. The total H_2O-to-alkoxide (TEOS + Zr−*n*-propoxide) molar ratios in the final sols were mantained in the range of 6−8. The *n*-propanol−*i*-propanol molar ratio in the sols was 2:1. Thoroughly cleaned silica glass (Heraeus) substrates were used for sol−gel dip-coating preparation. The withdrawal velocities of the substrates were in the range of 1.3−1.67 mm/s. The resulting films, deposited on silica substrate, were dried at 60 °C in air. Five sets of films of thicknesses ranging from 70 to 140 nm were synthesized. The general formula of the film is $(SiO_2)_x(ZrO_2)_{0.9-x}Ag_{0.1}$ (Table 1) in accordance with the sol compositions. In order to investigate the structure of the film matrix and the clusters growth as a function of the temperature, the samples were annealed at 200−900 °C for 30−60 min in air, N_2 and 5%H_2−95%N_2 (in the following indicated simply as H_2).

Table 1. Film Thickness and Composition Obtained by RBS on Mixed Ag-Doped SiO_2-ZrO_2 Systems after Annealing at 500 °C for 30 min in Air (in Brackets the Nominal Compositions)[a]

sample label	x SiO_2	film thickness (nm)	RBS composition (mol % ±5%)		
			Ag	SiO_2	ZrO_2
ZS10	0	65 ± 5	10 (10)		90 (90)
ZS31	0.225	75 ± 5	7.0 (10)	25.5 (22.5)	67.5 (67.5)
ZS22	0.450	85 ± 5	8.2 (10)	44.0 (45.0)	47.8 (45.0)
ZS13	0.675	110 ± 10	8.2 (10)	67.8 (67.5)	23.5 (22.5)
ZS01	0.9	140 ± 10	6.0 (10)	94.0 (90.0)	

[a] The samples are labeled according to the SiO_2 molar fraction x: for instance, ZS31 indicates three parts of ZrO_2 (Z) and one part of SiO_2 (S), whereas ZS10 indicates pure ZrO_2.

The composition of the films was determined by Rutherford backscattering spectrometry (RBS) by using a 2.2 MeV $^4He^+$ beam at National Laboratories INFN-Legnaro. Samples were 45° tilted in order to enhance the depth resolution. The refractive indices were determined from 350 to 800 nm with normal incidence transmittance and reflectance spectrophotometry, while the linear optical absorption spectra were measured in the wavelength region from 200 to 800 nm by using a Cary 5 dual-beam spectrophotometer. Microstructural and microanalytical characterization was performed by transmission electron microscopy (TEM) with a Philips CM30 T operating at 300 kV, equipped with an EDAX energy/dispersive spectrometer (EDS) and a GATAN parallel electron energy loss spectrometer (PEELS) at the CNR-LAMEL Institute in Bologna. The samples for electron microscopy were prepared as planar sections by indenting 3 mm disks with an ultrasonic drill, mechanically back-thinning down to an ∼20 μm thickness and Ar^+ ion-milling at 5 keV with ∼13° incidence, followed by a final step at 3 keV with rotating specimen so as to remove surface damage due to the main milling procedure.

(4) Kreibig, U.; Vollmer, M. *Optical properties of metal clusters*; Springer-Verlag: Berlin Heidelberg, 1995.
(5) Acosta, D.; Novaro, A.; López, T.; Gómez, R. *J. Mater. Res.* **1995**, *10*, 1397.
(6) Palladino, M.; Pirini, F.; Beghi, M.; Chiurlo, P.; Cogliati, G.; Costa, L. *J. Non-Cryst. Solids* **1992**, *147/148*, 335.
(7) Zevin, M.; Reisfield, R. *Opt. Mater.* **1997**, *8*, 37.
(8) Colomban, P.; Mazerolles, L. *J. Mater. Sci.* **1990**, *26*, 3503.
(9) De, G.; Gusso, M.; Tapfer, L.; Catalano, M.; Gonella, F.; Mattei, G.; Mazzoldi, P.; Battaglin, G. *J. Appl. Phys.* **1996**, *80*, 6734.

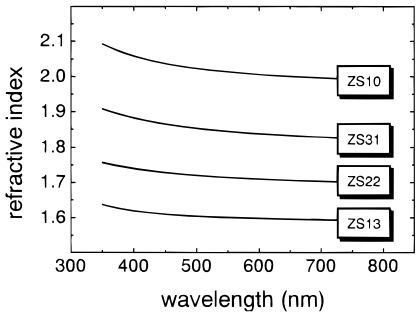

Figure 1. Refractive index as a function of the wavelength measured by normal incidence transmittance and reflectance spectrophotometry.

Table 2. Calculated (According to Equation 2) and Measured (by Spectrophotometry) Refractive Index for the Ag-Doped Mixed ZrO_2−SiO_2 Matrices

label	x_{SiO_2}	n_{calc}	n_{meas}
ZS10	0	2.0	2.01 ± 0.02
ZS31	0.225	1.865	1.84 ± 0.01
ZS22	0.450	1.730	1.71 ± 0.01
ZS13	0.675	1.595	1.60 ± 0.01

In order to prevent sample damage and artifacts induced by temperature rises during ion milling, the specimens were cryogenically cooled with liquid nitrogen.

3. Results and Discussion

The Rutherford backscattering technique has been used to determine composition and thickness of the mixed SiO_2−ZrO_2 films. The results are summarized in Table 1 and show a good agreement with the nominal values. It has to be noted that in the samples containing ZrO_2 RBS analysis also revealed the presence of about 1 mol % HfO_2 of the total ZrO_2.

In order to obtain the refractive indices of the samples, the normal incidence transmittance and reflectance spectrophotometric analysis has been carried out and the experimental data in the range 350−800 nm have been fitted by imposing a continuous set of solutions for the refractive index.[10,11] The results are reported in Figure 1. It is interesting to compare them with the refractive indices calculated on the basis of the sample stoichiometry, assuming that the index of the system can be described by the average weighted on the molar fraction of the indices of its components as the Beer−Gladston effective-medium theory:[4]

$$n_{tot} = xn_{SiO_2} + (1 - x)n_{ZrO_2} = 2.0 - 0.54x \qquad (2)$$

where we assumed $n_{SiO_2} = 1.46$ and $n_{ZrO_2} = 2.0$. Inserting the SiO_2 molar fraction x (normalized to 0.9 to take into account the 10 mol % of Ag) in eq 2, one obtains the calculated refractive indices reported in Table 2 together with the measured values of n averaged over the spectral range considered. The agreement is very good for all the systems investigated, suggesting that there is a separation of the ZrO_2 and SiO_2 subsystems instead of an alloying between them.

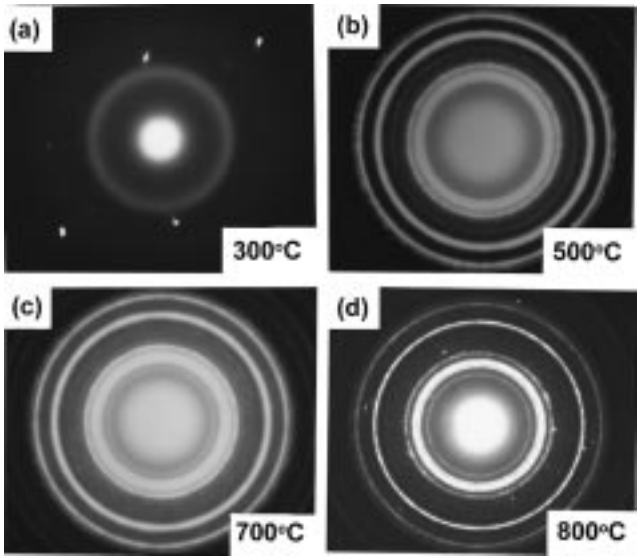

Figure 2. SAED patterns of the sample ZS10 (90%ZrO_2−10%Ag) annealed at (a) 300 °C in air, (b) 500 °C in air, (c) 700 °C in N_2, and (d) at 800 °C in H_2.

3.1. Ag Clusters in Pure ZrO_2. 3.1.1. TEM. In order to investigate the structure of the ZrO_2 matrix and the clusters growth as a function of the temperature, the sample ZS10 was annealed for 30 min in the temperature range 200−900 °C.

The phase diagram indicates that bulk pure zirconia undergoes a phase transition from monoclinic ($P2_1/c$ space group) to tetragonal ($P4_2/nmc$) around 1200 °C and to cubic ($Fm3m$) around 2370 °C.[12,13] It is also known that the sol−gel technique produces pure ZrO_2 in the (metastable) cubic or tetragonal phase at lower temperatures around 400−500 °C.[14,15] Above such temperatures the system evolves in the monoclinic phase, which remains stable up to about 1100 °C.[5] Nevertheless, as pointed out in refs 5 and 15, such evolution is highly sensitive to the preparation condition and possible stabilization of coexisting phases can occur when the size of the crystallites is of the order of 50 nm or below. We found a similar trend in the evolution of the structure as a function of the temperature, although our samples are slightly different from simply pure ZrO_2 due to the presence of 10% M Ag. The results of TEM analysis for the ZrO_2:Ag system as a function of the annealing temperature are summarized in Figure 2 and 3. In particular, from the selected area electron diffraction (SAED) analysis of Figure 2, we observe that the sample ZS10 annealed at 300 °C in air, Figure 2a, shows an amorphous pattern with two halos whose maxima approximatively correspond to the [111] and [220] reflections of the cubic ZrO_2. Moreover, some spots which can be consistently attributed to Ag fcc crystallites are present: these are due to large (100−200 nm diameter) and irregularly shaped Ag clusters, which are clearly visible in the corresponding bright-field (BF)

(10) Montecchi, M. *Pure Appl. Opt.* **1995**, *4*, 831.
(11) Anderson, C.; Arnold, G. W.; Bange, K.; Baucke, F.; Colombo, P.; Della Mea, G.; Dran, J. C.; Emiliani, G.; Geotti Bianchini, F.; Kawahara, H.; Leuhede, P.; Maddalena, A.; Manocha, A. S.; Matzke, H. J.; Matzumoto, H.; Mazzoldi, P.; Noshiro, M.; Polato, P.; Principi, G.; Rigato, V. *Glass Technol.* **1996**, *37*, 204.
(12) Massalski, T., Murray, J., Bennett, L., Baker, H., Eds.; *Binary Alloy Phase Diagrams*; American Society for Metals: Metals Park, OH, 1986.
(13) Uchikoshi, T.; Sakka, Y.; Ozawa, K.; Hiraga, K. *J. Mater. Res.* **1998**, *13*, 840.
(14) Atta, A. K.; Biswas, P. K.; Ganguli, D. *Thin Solid Films* **1991**, *197*, 187.
(15) Jana, S.; Biswas, P. K. *Mater. Lett.* **1997**, *30*, 53.

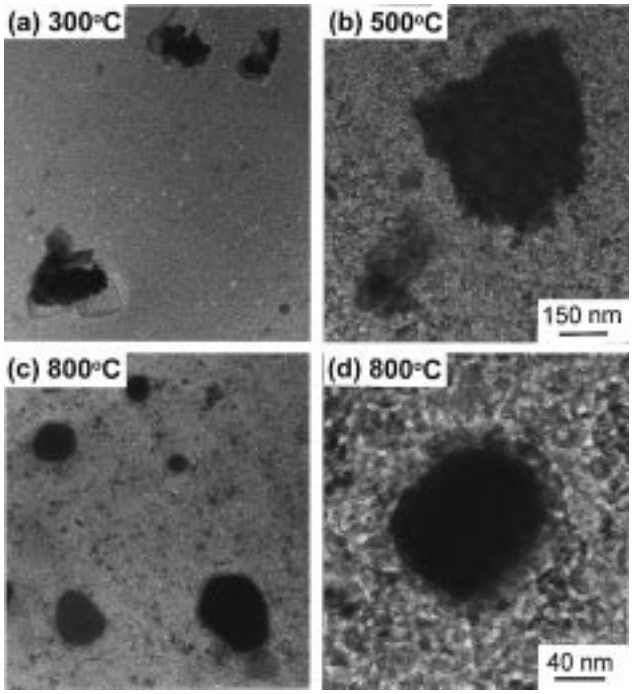

Figure 3. BF TEM micrograph planar views of the sample ZS10 (90%ZrO_2−10%Ag) annealed at (a) 300 °C in air, (b) 500 °C in air, (c) 800 °C in H_2 (all at the same magnification), and (d) at 800 °C in H_2 (higher magnification).

TEM micrograph, Figure 3a and whose composition has been measured by EDS microanalysis. The structural evolution of the ZrO_2 matrix as a function of the temperature can be seen in Figure 2b for the samples annealed at 500 °C in air. The Debye−Scherrer rings of the polycrystalline structure are clearly visible, showing the coexistence of cubic and tetragonal phases. Some weak rings characteristic of the monoclinic phase (in particular those arising from [011] planes) start to develop, indicating that a phase transition is taking place. Indeed, either the sample ZS10 annealed in N_2 at 700 °C, Figure 2c, or in H_2 at 800 °C, Figure 2d, shows the monoclinic phase, along with the two more symmetric cubic and tetragonal structures. A comparison of the diffracted intensities of the three phases is found in Figure 4, which reports kinematical simulation of the SAED Debye−Scherrer rings for ZrO_2. The presence in the SAED pattern of strong reflections from the crystalline matrix tends to hinder the visibility of the silver fcc ones which are very weak because of the molar ratio 1:9 almost overlapping with the previous ones, as indicated in Figure 4c by vertical arrows.

Looking at the structure of the system with BF and dark-field (DF) imaging modes, it is possible to evidence that the polycrystalline matrix is composed of mutually randomly oriented crystallites, whose dimensions estimated by high-resolution TEM (HRTEM) are ∼10−30 nm, in agreement with TEM and XRD measurements of ref 16 in pure sol−gel ZrO_2. This could be responsible for the stabilization of the higher-temperature cubic and tetragonal phases. It is interesting to note that in the samples annealed at 800 °C in H_2 some structures (∼100 nm large and irregularly shaped) are present whose

(16) Vesteghem, H.; Lecomte, A.; Dauger, A. *J. Non-Cryst. Solids* **1992**, *147/148*, 503.

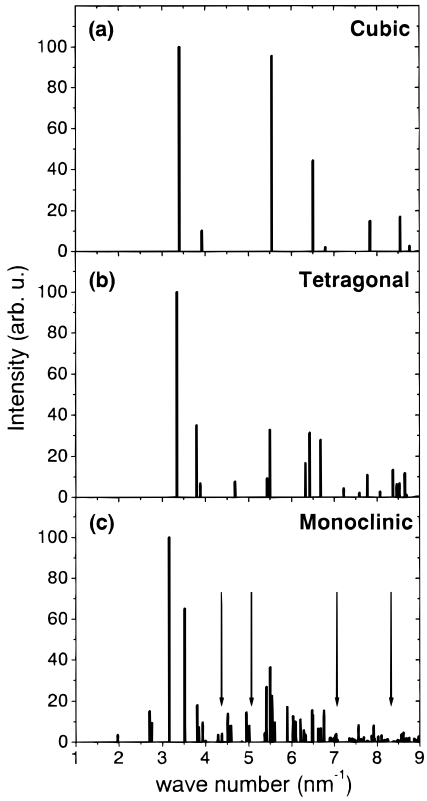

Figure 4. Kinematical simulation of the SAED pattern for ZrO_2 in its most common phases: (a) cubic, (b) tetragonal, and (c) monoclinic. The intensity of the strongest reflections are normalized to 100. Vertical arrows in (c) indicate the fcc reflections of Ag.

composition determined by EDS and PEELS analysis is consistent with the formation of $ZrSiO_4$ probably as a byproduct of the reaction of ZrO_2 with the SiO_2 substrate.

As far as the Ag cluster growth is concerned, it has to be pointed out that in all the samples examined some very large crystalline clusters (up to ∼300 nm in diameter) are detected. As evidenced by Figure 3 the shape of such clusters tends to become more regular as the annealing temperature increases. A closer inspection of the BF image of such clusters shows the presence of a well-defined shell (few nanometers thick) around them (see Figure 3d), whose composition is up to now not well-understood and which suggests that possible chemical interaction of silver with the ZrO_2 matrix takes place.

By means of EDS compositional analysis one can find a clear Ag signal also in regions of the matrix where such big clusters are not present. This is consistent with the occurrence of smaller silver particles but it is difficult to unambiguously locate their position because their contrast is overwhelmed by the interwoven contribution arising from the crystallites forming the matrix. Nevertheless, the fact that Ag clusters are present is evidenced by SAED and EDS compositional analysis. In addition, in BF and HRTEM imaging modes some spherical clusters of about 10 nm diameter are visible against an interconnected background of ZrO_2 crystallites[16] as one can see in the BF image of Figure 3.

3.1.2. Optical Absorption. The absorption spectra of the ZrO_2:Ag sample annealed for 1 h in H_2 at different temperatures are reported in Figure 5. Two main

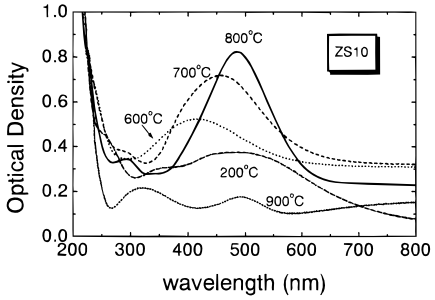

Figure 5. Optical absorption spectra of the ZrO_2:Ag system annealed in H_2 for 1 h at different temperatures.

features may be evidenced in the as-grown sample (annealed at 200 °C): a shoulder near 270 nm which can be ascribed to the matrix[15,17] and a very broad absorption peak with maximum at 482 nm probably induced by silver. When the annealing temperature reaches 500−600 °C the main absorption band blue-shifts and the resulting maximum is located at 419 nm. Theoretical calculations based on the Mie theory can explain such a shift only assuming a reduction to about $n = 1.8$ of the refractive index of the host with respect to the pure zirconia value of $n = 2$. This is at variance with the measured value of the ZS10 sample annealed at the same temperature but in air, as shown in Table 2. We can attribute this behavior to two possible mechanisms: the first is related to the nature of the cluster−matrix interface. The different chemical properties of silver and zirconia imply the possibility of defects around the cluster which develop as a locally enhanced porosity between cluster and matrix, as suggested in ref 18. Therefore, the dielectric screening of the host could be reduced by this local effect, promoting a blue-shift of the overall optical response which is on a phenomenological ground equivalent to reducing the refractive index of the matrix. The second mechanism could be related to the complex structural evolution of the matrix as the temperature is increased. Indeed, considering that, as evidenced by TEM analysis, above 300 °C an amorphous-to-crystalline transition takes place with subsequent phase transitions, which are accompanied by large volume changes,[13] it is also possible that different structural arrangements can be obtained with different annealing conditions, leading to different dielectric properties. It is likely that when the temperature is high enough, all these defects can be annealed out, restoring the theoretically expected dielectric behavior of the cluster−matrix interface. Indeed, when the annealing temperature is raised further at 700 °C in H_2, the absorption band maximum increases its intensity and red-shifts again ($\lambda_{max} = 458$ nm), reaching the value of 487 nm at 800 °C, which is precisely the Mie SPR for Ag clusters in ZrO_2. We have compared the effect of inert annealing (N_2) at the same temperatures on such samples: the results show that cluster precipitation is more effective in the case of reducing (H_2) atmosphere at the same temperature, confirming the results of ref 19. When the temperature

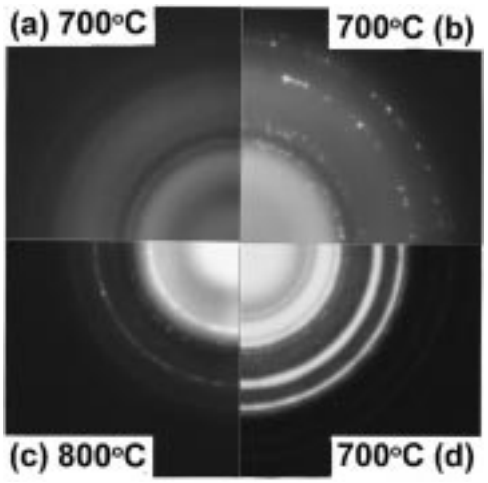

Figure 6. SAED patterns of the sol−gel synthesized mixed ZrO_2:SiO_2 matrices doped with Ag clusters and annealed at 700 °C: (a) ZS31 in H_2 and ZS22 in N_2, (b) ZS13 in H_2, (c) ZS22 in H_2 but annealed at 800 °C, and (d) ZS10 in N_2.

reaches 900 °C, the Ag absorption band disappears, suggesting that as already observed in ref 9 a melting of the silver clusters took place below the bulk melting temperature (which is at 962 °C) as a consequence of the thermodynamic size-effect.[20]

3.2. Ag Clusters in Mixed ZrO_2−SiO_2. 3.2.1. TEM. The situation is substantially different when the SiO_2 is added to the ZrO_2 matrix. As pointed out in ref 9, when dealing only with SiO_2 as the host, the sol−gel synthesized matrix is found to be always amorphous and the only crystalline reflections belong to embedded metallic clusters. This tendency toward amorphous arrangements of SiO_2 counteracts the ZrO_2 ability to form crystalline networks: all the examined samples with different ZrO_2/SiO_2 ratios gave upon final annealing at 700 °C an amorphous SAED pattern, on which the fcc rings of silver particles are now clearly visible. The comparison of the SAED patterns arising from the ZrO_2:SiO_2 samples annealed at 700 °C is reported in Figure 6. The samples ZS31 and ZS22 show similar spectra (Figure 6a) in which fcc Ag rings are present along with two diffuse bands whose wavevectors correspond to the [111] and [$\bar{2}$20] reflections of ZrO_2. In Figure 6b the SAED pattern of the sample ZS13 annealed in H_2 shows, in addition to the silver fcc spotty pattern, the presence of extra spots that, as already mentioned, can be ascribed to [111] ZrO_2 reflections. This suggests that possible ZrO_2 crystalline nucleation can take place upon increasing the annealing temperature. This has been actually observed by TEM for instance in the sample ZS22 annealed in H_2 at 800 °C, as shown by its SAED in Figure 6c, where the rings of the zirconia cubic phase are clearly visible. Just for comparison, we report also in Figure 6d the SAED results of ZS10 annealed in N_2 at 700 °C, which shows the polycrystalline nature of the matrix. The structural evolution of the matrix from amorphous to crystalline in the sample ZS22 around 800 °C is visible also in the BF micrograph of Figure 7, which shows the transition

(17) Morell, G.; Katiyar, R. S.; Torres, D.; Paje, S. E.; Llopis, J. *J. Appl. Phys.* **1997**, *81*, 2830.
(18) Palpant, B.; Prével, B.; Lermé, J.; Cottancin, E.; Pellarin, M.; Treilleux, M.; Perez, A.; Vialle, J. L.; Broyer, M. *Phys. Rev. B* **1998**, *57*, 1963.
(19) Marchi, G. D.; Caccavale, F.; Gonella, F.; Mattei, G.; Mazzoldi, P.; Battaglin, G.; Quaranta, A. *Appl. Phys. A* **1996**, *63*, 403.
(20) Kofman, R.; Cheyssac, P.; Aouaj, A.; Lereah, Y.; Deutscher, G.; Ben-David, T.; Penisson, J.; Bourret, A. *Surf. Sci.* **1994**, *303*, 231.

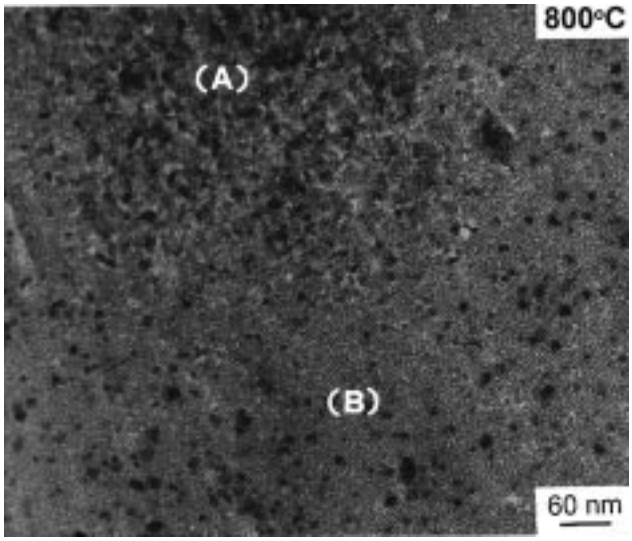

Figure 7. BF TEM micrograph of the sample ZS22 annealed in H_2 at 800 °C: the developing zirconia cubic phase is in the island labeled (A) against the amorphous background of the mixed ZrO_2:SiO_2 matrix (B).

region between the amorphous ZrO_2:SiO_2 matrix (B) and a growing polycrystalline island labeled (A) which exhibits upon diffraction the ZrO_2 cubic phase. This observed tendency of the ZrO_2:SiO_2 system to crystallize near 800 °C is in agreement with XRD measurements on similar samples,[6] which found that upon annealing, the tetragonal ZrO_2 phase builds up from the amorphous one with enhanced efficiency as the ZrO_2/SiO_2 molar fraction is increased. However, as pointed out in ref 6 such crystallization is remarkably process-dependent, so possible deviation in the crystallization temperature and phase can occur.

Despite the close similarity of the diffraction spectra for samples ZS31 and ZS22, minor differences have to be noticed regarding their Ag clusters distribution, as one can see in Figure 8, which reports the BF TEM images of the samples annealed at 700 °C. In the sample ZS31, annealed in H_2 for 1 h (Figure 8a), quite sparse 5−10 nm in diameter clusters are present with occasionally some bigger ones (∼30 nm), which produces the SAED pattern of fcc silver on the amorphous background: the average diameter obtained by TEM is $\langle d \rangle = 8 \pm 5$ nm. The situation is similar in the sample ZS22 annealed in N_2 for 30 min (Figure 8b) in which the clusters are denser in the matrix with respect to ZS31: a narrower size distribution is obtained with $\langle d \rangle = 7 \pm 3$ nm. The BF image (Figure 8c) of the sample ZS13 (annealed in H_2 for 1 h) indicates on the contrary a very broad size distribution of the Ag clusters: their diameters range from 5 nm up to even 80 nm, resulting in an averaged value of $\langle d \rangle = 20 \pm 19$ nm. In addition, the smaller particles have spherical shape whereas the biggest ones show different shapes (elongated, elliptical, and icosahedral) and structural defects (twins, for instance). Moreover, they present the same few nanometers thick shell around them, which we observe in the ZS10 sample, as stated above. The size distribution obtained by TEM analysis of the clusters diameters is reported in Figure 9 with the resulting mean diameters.

In order to corroborate the picture arising from the spectrophotometric analysis, that is, that the ZrO_2 and SiO_2 oxides preserve their own structure even if mixed

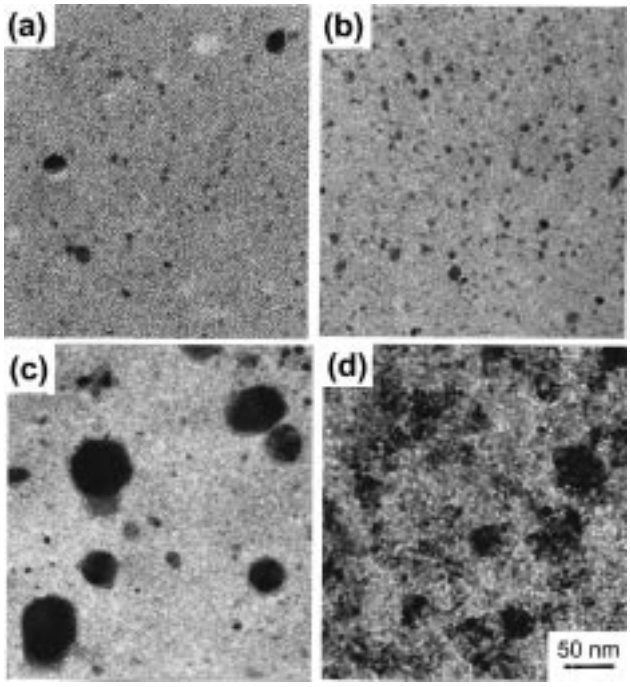

Figure 8. BF planar views of the sol−gel-synthesized mixed ZrO_2:SiO_2 matrices doped with Ag clusters and annealed at 700 °C: (a) ZS31 in H_2, (b) ZS22 in N_2, (c) ZS13 in H_2, and (d) ZS10 in N_2.

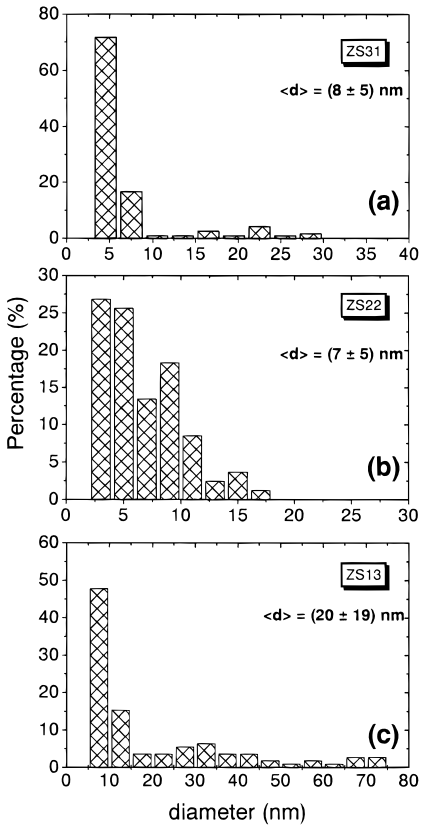

Figure 9. Histogram of size distribution in the mixed ZrO_2:SiO_2 samples annealed at 700 °C.

on a very fine size scale, we have performed PEELS measurements of the dielectric loss of the samples. The results are reported in Figure 10 which shows a comparison of the low-loss portion of the spectrum after deconvolution with the zero-loss peak to have a direct

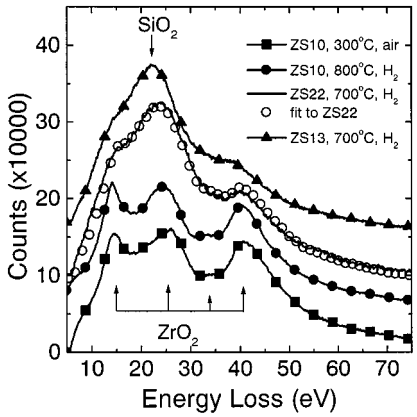

Figure 10. PEELS low-loss spectra (single scattering contribution) of the sol−gel-synthesized mixed ZrO_2:SiO_2 matrices doped with Ag clusters. Open circles refer to a linear fit to the spectrum of ZS22 annealed at 700 °C in H_2.

comparison of the single scattering contribution.[21] The spectra were taken at 300 keV in diffraction mode with a 0.2 eV/channel energy dispersion. In order to better follow the evolution of the spectra as a function of the matrix composition the curves are vertically shifted, with vertical arrows indicating the most relevant features in the spectrum of the bulk SiO_2 and ZrO_2. As far as the ZS10 samples are concerned, only minor differences can be evidenced from the low-temperature (amorphous structure) and the high-temperature (polycrystalline) ones. When SiO_2 is added to the matrix, the main features of ZrO_2 gradually fade and the spectrum transforms in pure SiO_2. Open circles refer to a linear fit of the ZS22 spectrum, combining with equal weight the loss function of SiO_2 and ZrO_2. Without resorting to more sophisticated effective-medium theories reported, for instance, in ref 22, the quality of fit confirms that the spectrum can be modeled as a simple average of the dielectric loss functions of the two oxides. This shows that, at least for the amorphous SiO_2:ZrO_2 systems investigated, one can imagine the two oxide networks as separated although interpenetrated.

3.2.2. Optical Absorption. As far as the optical properties of the mixed systems are concerned, the measured absorption spectra show a complex evolution of the main resonances as a function of the H_2-annealing conditions, as reported in Figure 11. At variance with the sample ZS10, the spectra do not exhibit large variations in the SPR position as a function of the annealing temperature: instead, we observe only a sharpening of the absorption band as the temperature reaches 700−800 °C before it disappears around 800−900 °C, indicating the onset of cluster melting below the silver bulk melting temperature. There is a good agreement with the measured spectra (solid lines) and the ones calculated with Mie theory (represented by the curves with hollow circles), assuming the size distributions obtained by TEM data and the refractive indices measured by spectrophotometry. With regard to the SPR position the optical data show a clear red-shift as the refractive index of the host is reduced, as summarized in Table 3. This shows that apart from controlling the exact size distribution of the clusters (which reflects in the amplitude of the SPR resonance) it is possible to control the position of the resonance by changing the matrix composition.

(21) Egerton, R. F. *Electron Energy-Loss in the Electron Microscope*; 2nd ed.; Plenum Press: New York, London, 1996.

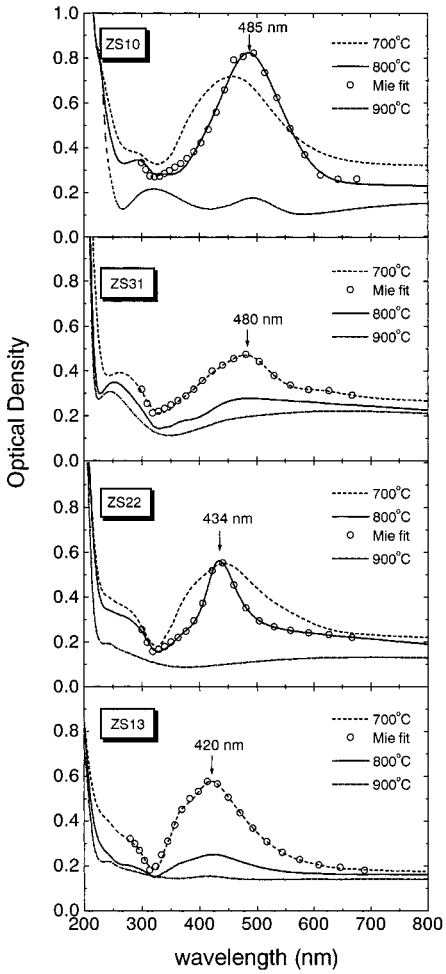

Figure 11. Optical absorption spectra of the mixed ZrO_2:SiO_2 matrices doped with Ag clusters as a function of the composition and the annealing temperature. Open circles are fits obtained with Mie calculations and a size distribution obtained by TEM.

Table 3. Evolution of the SPR Peak Position as a Function of the Matrix Composition

label	x_{SiO_2}	SPR (nm)
ZS10	0	485
ZS31	0.225	480
ZS22	0.450	434
ZS13	0.675	420
ZS01	0.9	410

4. Conclusions

In this work we have studied the structural and optical properties of sol−gel-derived Ag-doped mixed SiO_2:ZrO_2 matrices. The complex structural evolution of a pure ZrO_2 matrix has been followed by TEM, indicating the stabilization of high-temperature cubic and tetragonal phases induced by the small size of the crystallites forming the matrix. This ability to form a crystalline network can be controlled by adding increasing amounts of SiO_2 to the system, which shifts toward higher temperatures the threshold for amorphous to polycrystalline transition which is around 400 °C for ZrO_2 and 800 °C for mixed systems, respectively. Spec-

trophotometric and EELS analysis allowed us to conclude that the SiO_2 and ZrO_2 networks are well-separated even if mixed at a fine size scale. No evidence for zircon ($ZrSiO_4$) formation has been found in the mixed system, at least in the temperature range investigated. The presence of well-defined Ag clusters has been evidenced by TEM and optical measurements, indicating that the different ZrO_2/SiO_2 molar ratios result in different average diameters and size dispersions, suggesting that both structural and optical properties can be controlled by optimizing the growth process.

Acknowledgment. This work has been partially supported by M.U.R.S.T. (University and Research Ministry) within a National University Research Project.

CM980749X

(22) Howie, A.; Walsh, C. *Microsc. Microanal. Microstruct*. **1991**, *2*, 171.